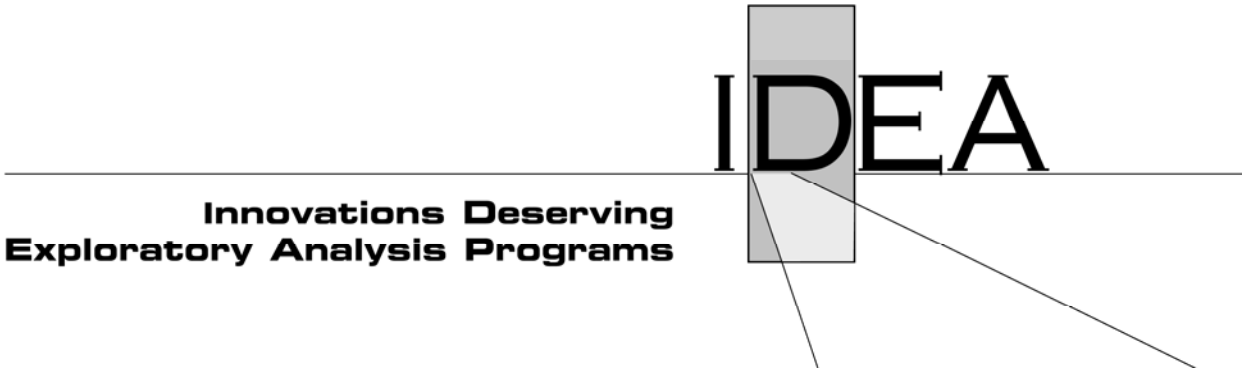

High-Speed Rail IDEA Program

HIGH-PRECISION GPS FOR CONTINUOUS MONITORING OF RAIL

Final Report for High-Speed Rail IDEA Project 26

Prepared by:
David C. Munson
Coordinated Science Laboratory and
Department of Electrical and Computer Engineering
University of Illinois, Urbana-Champaign

February 2004

TRANSPORTATION RESEARCH BOARD
OF THE NATIONAL ACADEMIES

INNOVATIONS DESERVING EXPLORATORY ANALYSIS (IDEA) PROGRAMS MANAGED BY THE TRANSPORTATION RESEARCH BOARD

This investigation was performed as part of the High-Speed Rail IDEA program supports innovative methods and technology in support of the Federal Railroad Administration's (FRA) next-generation high-speed rail technology development program.

The High-Speed Rail IDEA program is one of four IDEA programs managed by TRB. The other IDEA programs are listed below.

- NCHRP Highway IDEA focuses on advances in the design, construction, safety, and maintenance of highway systems, is part of the National Cooperative Highway Research Program.
- Transit IDEA focuses on development and testing of innovative concepts and methods for improving transit practice. The Transit IDEA Program is part of the Transit Cooperative Research Program, a cooperative effort of the Federal Transit Administration (FTA), the Transportation Research Board (TRB) and the Transit Development Corporation, a nonprofit educational and research organization of the American Public Transportation Association. The program is funded by the FTA and is managed by TRB.
- Safety IDEA focuses on innovative approaches to improving motor carrier, railroad, and highway safety. The program is supported by the Federal Motor Carrier Safety Administration and the FRA.

Management of the four IDEA programs is integrated to promote the development and testing of nontraditional and innovative concepts, methods, and technologies for surface transportation.

For information on the IDEA programs, contact the IDEA programs office by telephone (202-334-3310); by fax (202-334-3471); or on the Internet at http://www.trb.org/idea

IDEA Programs
Transportation Research Board
500 Fifth Street, NW
Washington, DC 20001

HIGH-PRECISION GPS FOR CONTINUOUS MONITORING OF RAIL

IDEA Program Final Report
for the Period June 27, 2001 Through March 30, 2003
DOT Agreement DTFH61-00-X-0005

Prepared for
the IDEA Program
Transportation Research Board
National Research Council

David C. Munson
Coordinated Science Laboratory and
Department of Electrical and Computer Engineering
University of Illinois, Urbana-Champaign

Revised February 6, 2004

ABSTRACT

Estimation of rail position and geometry using high-precision differential GPS can be used to monitor the movement of rail. Because rail naturally expands and contracts during temperature changes, lack of movement during severe temperature change would indicate significant rail stress. Point-specific monitoring can detect slippage of rail down a mountainside or other longitudinal rail movement. High-accuracy measurements might be useful for a variety of future rail applications, including identifying buckle precursors and predicting rail failure. Measurements collected from a moving platform would be most practical for mapping long sections of rail.

In this study we compared raw and post-processed GPS trajectory measurements, collected from a high-railer, to stationary benchmark points. Our GPS system had an average error distance of 5-10 cm to the benchmark points. However, there was some calibration error and position variation between the GPS antenna and the rail; this error could be reduced with a more advanced system setup. The bulk of the error came from problems with GPS kinematic convergence. Because of integer ambiguities in the carrier signal, the GPS receiver does not always reliably estimate the correct number of carrier frequency cycles between the receiver and satellites. For short track segments, the integer ambiguity is observed as a constant bias in the data. A least-squares offset was calculated to remove this bias. Signal processing smoothing methods removed some of the inherent jaggedness of the trajectory data. After smoothing and bias removal, many of the trajectory measurements had an average error distance of about 1-2 cm to the stationary benchmark points. This reduced error is what might be achieved if the integer cycle ambiguity problem can be well solved.

GPS technology could potentially be used to detect geometric precursors to rail buckles, if such precursors exist. This report presents a buckle detection model that takes as input a rail trajectory corrupted by measurement noise and computes the probability that a low amplitude sinusoidal mode can be identified in the measurement data. We find that a GPS system operating at 3 cm accuracy could reliably find a low amplitude sinusoidal mode having amplitude 5-10 cm across a 50 m section

KEY WORDS

GPS, rail position estimation, integer cycle ambiguity resolution, buckle detection

TABLE OF CONTENTS

Executive Summary 1

Introduction 3

Data Collection 3
- Equipment Setup 3
- Cold Weather and Warm Weather Data 6

Analysis of Trajectory Runs 9
- Airport Trajectory Runs: Raw Data 9
- Airport Trajectory Runs: KIPPS-Processed 10
- Lake Trajectory Runs: Raw Data and KIPPS-Processed 12

Data Processing 13
- Offset of Kinematic Data from Benchmark Points 14
- KIPPS Offset Correction 15
- Smoothing of KIPPS Trajectories Before Offset Correction 17
- Smoothing of Raw Data Trajectories Before Offset Correction 19
- Other Data Processing Methods 20

Analysis of Rail Buckles 21
- Buckle Modeling 21

Accomplishments and Future Results 25

Appendix A: Antenna Calibration 27

Bibliography 28

EXECUTIVE SUMMARY

The goals of this study were to benchmark and enhance GPS system performance on a moving rail platform for the purpose of precisely measuring rail position. Such GPS measurements could be used to monitor rail movement due to temperature changes, heavy usage, bed deterioration, rail sliding, and track maintenance. Rail position measurements, combined with stress analysis, could be used to systematically find rail sections that have high levels of stress. These rail sections could then be checked more frequently for developing buckles and breaks.

Up to this point, a systematic analysis of GPS as a viable means of mapping rail trajectory has not been conducted. We believe that centimeter-level accuracy is necessary in order for GPS to be useful in detecting rail anomalies. Currently, there are GPS receivers on the market that tout accuracy as good as 2-3 mm from a stationary unit. However, for extensive rail networks, future applications would benefit most from a GPS system that can measure position quickly from a moving rail platform. This was the emphasis of our study.

Personnel from University of Illinois at Urbana-Champaign (UIUC) and Rockwell Collins tested a high-end GPS system mounted on a high-railer truck on sections of Cedar Rapids and Iowa City Railway (CRANDIC) track outside Cedar Rapids, IA. Trajectory data were collected on two different track geometries to determine the accuracy of measuring rail position under normal rail conditions. Two field tests were conducted in 2002 during cold and warm weather. Both stationary and moving measurements were made to test GPS as a reliable means of estimating rail location. These surveys were conducted on jointed rail. We had originally intended to make measurements on continuous welded rail (CWR), but these sections had considerable rail traffic or were in areas where GPS signal acquisition would have been more variable.

We found that moving GPS measurements do not dependably satisfy the error parameters needed for repeatable high-accuracy. Our GPS system had an average error distance of about 5-10 cm to the benchmark points. However, there was some calibration error and position variation between the GPS antenna and the rail; this error could be reduced with a more advanced system setup. The bulk of the error came from problems with GPS kinematic convergence. Because of integer ambiguities in the carrier signal, the GPS receiver might not reliably estimate the correct number of carrier frequency cycles between the receiver and satellites. A stationary system has the luxury of waiting until error correction algorithms can convergence upon a precise location. For a moving system, a more robust algorithm for integer estimation that can quickly converge to the right solution is needed. There is promising research being done in the area of phase unwrapping at UIUC, which could be applied to the GPS integer ambiguity problem. An algorithm that can reliably resolve the integer ambiguity can then be augmented with further signal processing enhancements to guard against losing lock during the run. Since rail is inherently smooth and the carrier phase measurements differ by wavelength multiples, post-processing can remove minor errant jumps in the trajectories.

For short track segments, the integer ambiguity is observed as a constant bias in the data. A least-squares offset was calculated to remove this bias. Signal processing smoothing methods removed some of the inherent jaggedness of the trajectory data. After smoothing and bias removal, many of the trajectory measurements had an average error distance of about 1-2 cm to the stationary benchmark points.

Location measurements for the benchmark points varied 1-2 centimeters between the cold and warm weather tests. Because the measurements were taken on jointed rail, the 1-2 centimeter differences may not have been due to rail movement. Instead, sources of error could have been from a slight tilt in the meter-high tripod holding the GPS antenna. Additionally, the tripod might not have been placed at the exact location of the previous measurement. A more advanced setup would mitigate these errors.

We envision a variety of future rail applications for high-precision GPS. GPS might be useful for identifying buckle precursors and to predict rail "failure" prior to actual failure. GPS could be used to detect slippage of rail down a mountain-side or other longitudinal rail movement. An optical reader could be used to read marks off the track to determine if specific points moved significantly since the last set of measurement points. Rail stress could be calculated by measuring the longitudinal expansion and contraction during temperature changes; lack of movement during severe temperature change would indicate significant rail stress. While a moving GPS system would be more useful, stationary measurements from stationary fixtures attached to the rail could be used for especially problematic rail sections.

GPS technology could potentially be used to detect geometric precursors to rail buckles. At this time, it is unknown whether such precursors exist. A database containing past trajectory measurements could show if there is movement prior to a rail buckle. If such precursors do exist, a buckle prediction system could be developed.

This report presents a buckle detection model that takes as an input a rail trajectory corrupted by GPS measurement noise. This model computes the probability that a low amplitude sinusoidal mode exists in the measurement data. This assumes that the buckle precursor would approximate the shape of the buckle itself. From these calculations, receiver operating characteristic (ROC) curves are used to determine the probability of detection vs. the probability of miss (or false positive). In our calculations, a GPS system operating at 3 cm accuracy could reliably find low amplitude sinusoidal modes having amplitude 5-10 cm across a 50 m section.

The success of high-precision GPS for rail applications hinges on the development of better processing algorithms to improve measurement repeatability. A major conclusion of our study is that the primary limiting factor in GPS measurement reliability is the need for better integer cycle ambiguity resolution (ICAR), not trajectory filtering as originally thought. We are now working on this critical problem. In the next few years, the addition of a new civilian GPS frequency will help simplify the ICAR problem.

INTRODUCTION

This report details work conducted on high precision measurement of rail position from a moving platform using the Global Positioning System (GPS).

Traditionally, GPS has been used for on-board, real-time precise location of rail vehicles and other rail assets. The purpose of this study was to determine if GPS might provide sufficient accuracy to monitor rail movement due to temperature changes, heavy usage, bed deterioration, rail sliding, and track maintenance.

Our first task was to benchmark existing GPS technology in order to characterize performance and identify opportunities for further research. The section on ***Data Collection*** summarizes our collection procedure and equipment setup on two sections of rail near Cedar Rapids, IA, during both cold and warm weather. Rockwell supplied both GPS equipment and personnel for those tests.

The ***Analysis of Trajectory Runs*** section provides an overview of the measurement data sets. After analyzing the collected data, we consider ways to improve the accuracy of the real-time kinematic trajectories with respect to benchmark points. An enhanced High-Precision GPS (HPGPS) is needed that would map rail location accurately to within a few centimeters. The section on ***Data Processing*** describe the signal processing techniques we used to improve accuracy of both raw and filtered data sets provided by Rockwell.

We also address how HPGPS might be used to detect onset of rail buckles. Potentially, better rail position measurements, combined with stress analysis would aid in systematically finding rail sections that have high levels of stress. These sections could then be checked more frequently for developing rail buckles or breaks in order to predict rail failure prior to actual failure. In the future, with the aid of an optical reader to read marks on the side of the rail, it should be possible to detect slippage of rail down a mountain-side or other longitudinal rail movement, and to calculate rail stress from longitudinal expansion and contraction. The ***Analysis of Rail Buckles*** section addresses issues in predicting rail buckles using rail geometry. The final section summarizes our findings and comments on future directions for this research project.

DATA COLLECTION

The GPS data was collected during two different field tests in 2002. During the initial planning phase, we decided on taking both cold and warm weather measurements to offer the possibility of detecting rail movement due to temperature changes. We also wished to test the GPS system on different track geometries. We selected two sections of Cedar Rapids and Iowa City Railway (CRANDIC) track outside Cedar Rapids, IA. Personnel from Rockwell and the University of Illinois at Urbana-Champaign (UIUC) were involved in collecting the GPS data.

The cold weather measurements were taken on Friday, February 22, 2002. The preceding day was used to meet with CRANDIC, select the track sections, inspect the high-railer, and ready the equipment. Of the two track sections selected, one was straight, adjacent to the Eastern Iowa Airport, and the other was curved, along the edge of Coralville Lake. The straight section was about 1800' long and the curved section was about 2300' long. These sections had jointed rail, but were attractive because they have little traffic and because they are ``out in the clear'' -- not heavily wooded as were other candidate sections considered, which might have provided more variable GPS signal acquisition.

For the straight section, we collected 6 moving data sets at low speed (about 5 mph) and 5 at higher speed (about 15 mph). For the curved section, we collected 3 data sets at low speed and 3 at higher speed. Benchmark, static GPS measurements were taken at intervals of about 150' along the rail, with a precision of three millimeters for each measurement

The temperature was 16 ^{o}F when we began setting up for the data collection. However, later in the morning and afternoon, the temperature rose to about 38 ^{o}F during the actual data collection. The rail temperature was about 52 ^{o}F on the shady side of the rail. These temperatures were higher than we would have liked, but the winter of 2002 was incredibly mild in the Midwest, so we were actually fortunate to get temperatures this low.

On July 29-30, we returned to Cedar Rapids to collect warm weather data at the same airport and lake sites. The air temperature was 88 ^{o}F and the rail temperature was 118 ^{o}F on the shady side of the rail. At both sites, we collected 10 moving data sets, 5 each at low and high speeds. The same benchmark points marked during the cold weather data collection were remeasured using stationary GPS to an accuracy of 4 mm and were used for the warm weather data analysis.

EQUIPMENT SETUP

A CRANDIC high-railer truck was used for the data runs. The GPS system inside the high-railer incorporated dual frequency (L1 and L2 bands) measurements from a GPS antenna placed on top of the high-railer and from an inertial navigation system (INS) unit inside the truck. Figure 1 shows the high-railer truck near Coralville Lake.

Figure 1 High-Railer Truck

GPS measurements were acquired at a 10 Hz rate, and the INS was used to generate position coordinates between the GPS readings using an inertial motion unit (IMU). The high-railer did not have a 12V supply that we could use, but fortunately, Rockwell was able to rig up portable 12V supplies to power the GPS equipment and computers. Figure 2 shows the GPS and IMU units inside the high-railer truck.

Figure 2 GPS units (left and middle) and IMU unit (right)

The GPS system used both kinematic and carrier-phase differential processing. Carrier-phase DGPS calculates range based on the carrier phase and is version of differential GPS (DGPS), which calculates position with respect to the position of the base station. True position coordinates were then estimated using the differential measurements plus the approximate position coordinates of the base station.

Usually, the term "kinematic" describes applications in which the position of a non-stationary object is determined. The term "kinematic GPS" used by Rockwell refers to kinematic surveying and carrier-phase measurement postprocessing. Although this is a slight misnomer, we will use Rockwell's definition of "kinematic GPS" for this report.

Since the base station coordinates were approximate, any future measurements in the same relative reference frame require that the same base station location be used. The location of the base station was marked with an iron stake at each test site. Figure 3 shows the base station antenna next to the van. The Eastern Iowa Airport can be seen in the background.

Figure 3 Van with Base Station Antenna

The benchmark surveys were conducted using two GPS receivers - one at the points to be surveyed and the other at the base station. All measurements were differential, made with respect to the base point. Figure 4 shows the setup of the survey antenna, which was used to acquired the positions of the benchmark points.

Figure 4 also shows the base of the survey antenna resting on a rail benchmark. The marks were placed at approximately 150' intervals along the rail. It was necessary for the survey antenna to remain stationary for several minutes at each survey point to provide 3-4 millimeter accuracy.

Figure 4 (a) Survey Antenna, and (b) Survey Mark

Antenna Testing Calibration

See Appendix A for a detailed explanation of the antennas used during the data collection.

Site Maps

Figure 5 shows the location of base station survey point used at the airport test site. Figure 6 shows the location of base station survey point used at the lake test site.

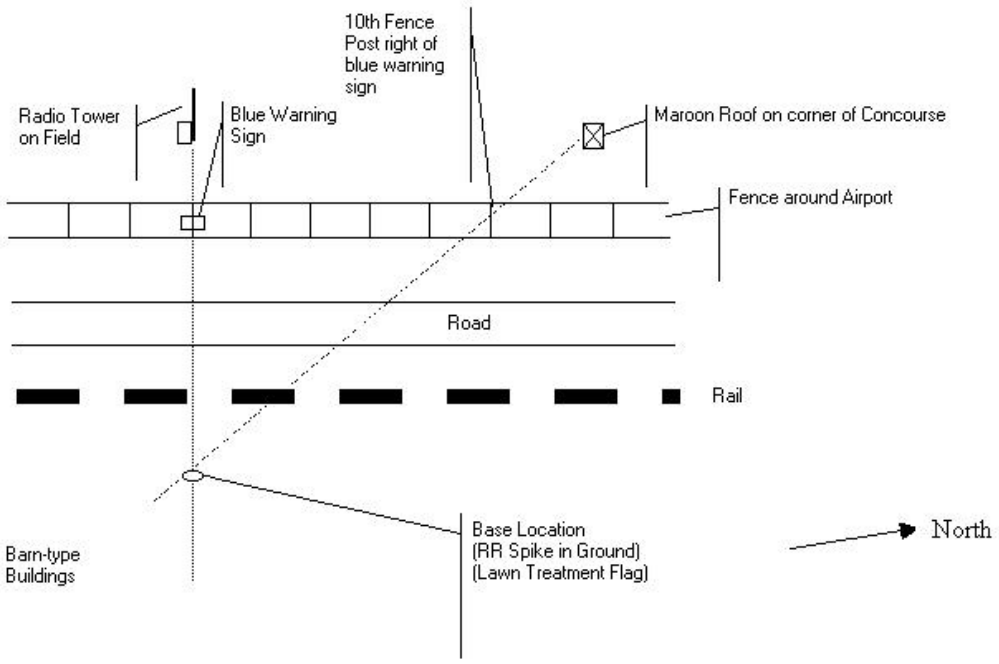

Figure 5 Airport Test Site

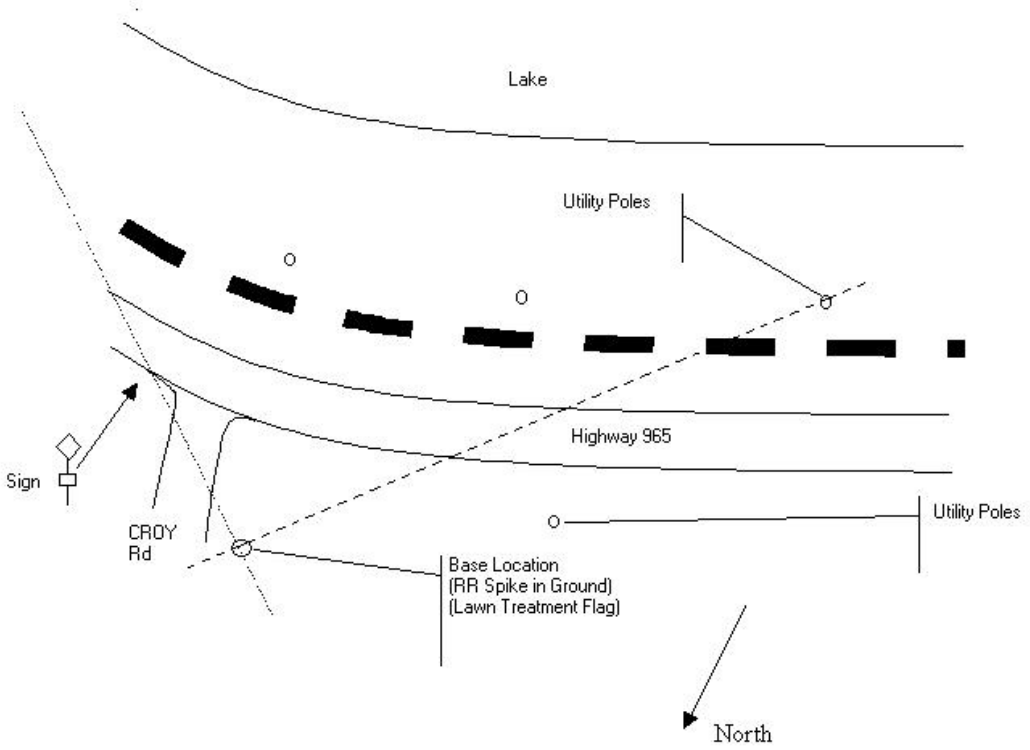

Figure 6 Lake Test Site

COLD WEATHER AND WARM WEATHER DATA

For both cold and warm weather tests, the base station locations were determined using self-survey mode in the Ashtech Z-12. Eleven benchmark points were collected at the airport site and fifteen were collected at the lake site. For each site, GPS data was collected at both 5 mph and 15 mph. At the airport site, two sets of data were collected - with and without

a stationary time of 5 minutes at the beginning of the run to calibrate the GPS receiver. The distance between the cold weather and warm weather benchmark points was as large as 3 cm, but generally less than 1 cm in the northing/easting (NE) coordinate frame. (GPS is generally less accurate in measuring altitude than in measuring position on the local tangent plane).

Table 1 and Table 2 provide a brief overview of the test runs performed. Runs A-F did not have a stationary time to calibrate the GPS receiver; later runs did include a calibration time. Comprehensive tables providing the measured coordinates for the benchmark points as well as run overviews can be viewed in *(1)*.

Cold Weather

Run	speed (mph)
A*	5
B*	5
C*	5
D*	15
E*	15
F*	15
G	5
H	5
J	5
I	15
K	15

Warm Weather

Run	speed (mph)
A1	5
A2	5
A3	5
A4	5
A5	5
A6	15
A7	15
A8	15
A9	15
A10	15

* no stationary time

Table 1 Airport Runs

Cold Weather

Run	speed (mph)
L	5
M	5
N	5
P	15
Q	15
R	15

Warm Weather

Run	speed (mph)
B1	5
B2	5
B3	5
B4	5
B5	5
B6	15
B7	15
B8	15
B9	15
B10	15

Table 2 Lake Runs

Data Files

Three different files were provided by Rockwell for each run: a "raw" data file, a file containing trajectory data filtered by Rockwell software, KIPPS (which uses a Kalman filter for trajectory estimation), and a file marking the various GPS receiver (and Rockwell filter) states used by KIPPS.

1) The **pva.csv** file provides the "raw" navigation solution. This solution is defined as the non-kinematic real-time navigation solution in earth-centered, earth fixed (ECEF) coordinates. This solution is based upon GPS/INS measurement inputs, and is referenced to the IMU. Table 3 shows the information contained in each line of the file.

Element	Name	Units
1	Time	Seconds
2	ECEF Position X	Meters
3	ECEF Position Y	Meters
4	ECEF Position Z	Meters
5	ECEF Velocity X	Meters/seconds

6	ECEF Velocity Y	Meters/seconds
7	ECEF Velocity Z	Meters/seconds
8	ECEF Acceleration X	Meters/seconds^2
9	ECEF Acceleration Y	Meters/seconds^2
10	ECEF Acceleration Z	Meters/seconds^2
11	Roll	Radians
12	Pitch	Radians
13	Heading	Radians
14	Roll Rate	Radians/seconds
15	Pitch Rate	Radians/seconds
16	Heading Rate	Radians/seconds

Table 3 pva.csv parameters

2) The **precise.csv** file provides the precise navigation solution. This solution is defined as the kinematic postprocessed navigation solution (KIPPS) in ECEF coordinates. In this context, "kinematic postprocessed" means that the trajectory data incorporates the measurements referred to in the **count.csv** file and uses Kalman filtering to improve trajectory estimation. This solution is based upon GPS/INS measurement inputs and is referenced to the position of the IMU. Table 4 shows the information contained in each line of the file.

Element	Name	Units
1	GPS Time	Seconds
2	Kinematic ECEF Position X	Meters
3	Kinematic ECEF Position Y	Meters
4	Kinematic ECEF Position Z	Meters

Table 4 precise.csv parameters

3) The **count.csv** file indicates which measurements KIPPS uses when producing a precise solution. Table 5 shows the information contained in each line of the file.

Element	Name	Units
1	GPS Time	Seconds
2	Pseudorange Measurements Incorporated	--
3	Carrier Phase Measurements Incorporated	--
4	Ambiguity Measurements Incorporated	--

Table 5 count.csv parameters

Each measurement column contains the number of satellite combinations incorporated in making the measurement (i.e. 7 combinations equals 8 satellites). In theory, the location of the receiver can be determined from 4 satellites. Three satellites are needed to provide the geometric range to the receiver and one satellite corrects for the offset between the receiver clock and the satellite system clock; the receiver already knows the time offset between the individual satellites. But in practice, the satellite signal becomes corrupted by noise, atmospheric delays, Doppler frequency shifts, and other sources of error. It is better to track as many satellites as possible when determining the receiver position in the field.

Incorporating GPS Corrections and Obtaining Kinematic Convergence

The accuracy of the GPS trajectory depends on which measurements in Table 5 are incorporated in the calculations.

Pseudorange measurements refer to the distance measurement based on the correlation of a satellite transmitted code and the local receiver's reference code. Pseudorange has not been corrected for errors in synchronization between the transmitter's clock and the receiver's clock. Eventually, the navigation process learns this synchronization error as a by-product of the GPS navigation solution. GPS satellites use direct sequence spread spectrum (DSSS) modulation; this modulation technique uses codes similar to random binary sequences, but that are actually deterministic; these pseudorandom noise (PRN) codes are useful for low signal-to-noise applications. Commercial receivers often use a PRN code called course/acquisition (C/A) code to determine the range to the transmitting GPS satellite.

To improve accuracy, the carrier signal is incorporated into the data analysis. Although most GPS receivers use the time codes that are transmitted by the satellites for both position determination and for time transfer, it is also possible to use the carrier itself for similar purposes. Since the frequency of the carrier is about 1000 times higher than the frequency

of the C/A code, carrier phase measurements have much greater resolution, in principle. (L1 wavelength is approximately 19 cm and L2 wavelength is approximately 24 cm). To achieve better resolution, it is usually necessary to analyze the received data using postprocessed ephemeredes of the satellites (predictions of satellite positions and velocities from data transmitted by the GPS satellites) and detailed models of the ionosphere and troposphere. Fortunately, such models exist and it is possible to estimate position to an accuracy of 1% of the carrier wavelength (within a few millimeters!) with some receivers in the marketplace.

However, the overall phase measurement contains an unknown number of carrier-cycles between the satellites and receiver. This ambiguity exists because the receiver merely begins counting carrier cycles from the time the receiver locks onto the carrier phase. This issue is commonly referred to as integer cycle ambiguity resolution (ICAR). While there are methods that attempt to resolve this ambiguity using the geometry and path of the satellites and the receiver, this is not a completely solved problem and integer cycle ambiguities can hinder repeatability of measurements. For dual-band receivers, having both L1 and L2 frequencies does make the ICAR search more efficient because the sum and difference wavelengths can be exploited; however, the noise factor for the difference wavelength (wide-lane) processing does increase markedly *(2)*. The addition of a new civilian GPS frequency in the next few years will help simplify the ICAR problem. By introducing new wide-lane frequency combinations, the effects of noise can be mitigated, making it much easier to find the correct integer values.

Ambiguity resolution involves three major steps. The first step is the generation of potential integer ambiguity combinations that should be considered by the algorithm. A combination is composed of an integer ambiguity for, e.g., each of the double-difference satellite pairs. In order to determine these combinations, a search space must be constructed. The second major step is the identification of the correct integer ambiguity combinations. Many methods use a least-squares minimization approach. The third step is the validation (or verification) of the ambiguities *(3)*. Ambiguity resolution is a major problem with HPGPS. Improving performance is not trivial; it involves many issues beyond the scope of this report, and which require further research.

"Kinematic convergence" occurs when KIPPS picks a "track" that it believes corresponds to the correct number of carrier cycles between the satellites and receiver. This convergence is denoted in Table 5 when both carrier cycle and ambiguity measurements are incorporated in the postprocessing.

ANALYSIS OF TRAJECTORY RUNS

The figures in this section show representative trajectories (solid curve) and benchmark points (*) at the airport and lake sites.

For the cold weather tests, two sets of runs were collected at the airport site - with and without a stationary time of 5 minutes at the beginning of the run to calibrate the GPS receiver. For the warm weather tests, in order to take into account the problems encountered during the cold weather test runs, we decided to change the data collection procedure to allow more time for kinematic convergence. Instead of starting at the beginning of the rail section, the high-railer started collecting data at the end of the section. After waiting 5 minutes to calibrate the GPS receiver, the rail-higher backed up to the start of the track before moving forward for the data runs.

AIRPORT TRAJECTORY RUNS: RAW DATA

Figure 7 shows representative cold weather raw data trajectories for the airport site. Figure 8 shows representative warm weather raw data trajectories.

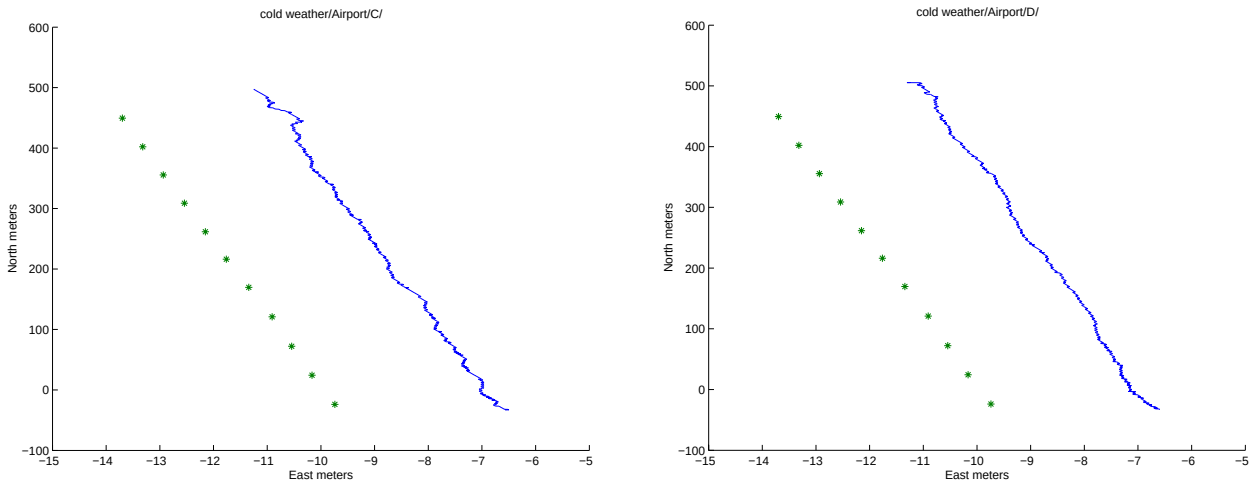

Figure 7 Representative cold weather raw data trajectories, airport runs, (a) 5 mph, and (b) 15 mph

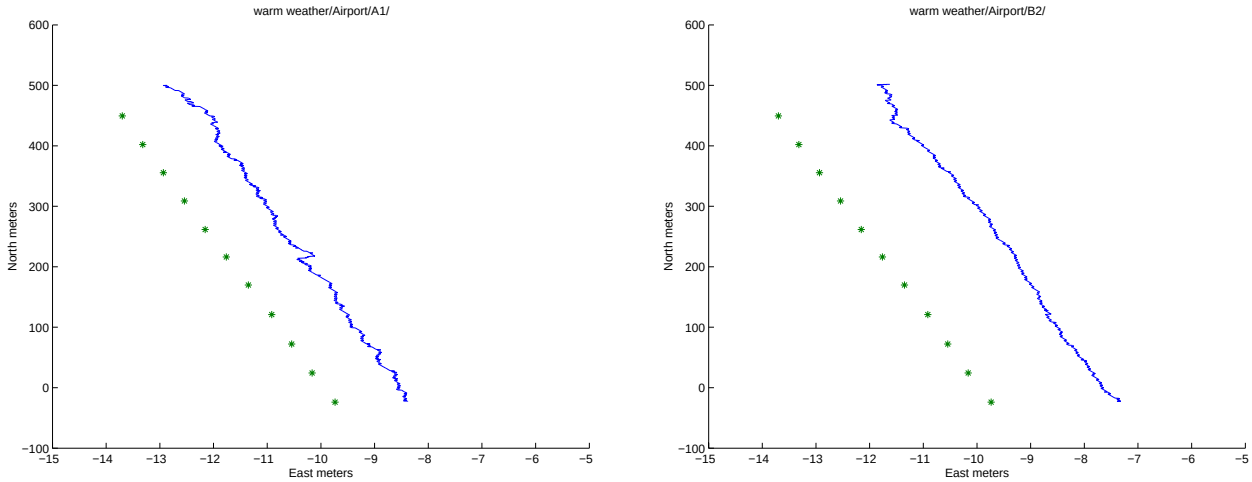

Figure 8 Representative warm weather raw data trajectories, airport runs, (a) 5 mph, and (b) 15 mph

The distance offset between the raw data trajectories and the benchmark points is expected, since without KIPPS processing (which provides integer cycle ambiguity resolution), the difference can be significant. Also, the trajectory measurements were based off the IMU inside the high-railer, while the benchmark points were measured at the base of the rail. The IMU sat in the high-railer almost directly above the rail base; the IMU was 1.21 m above and 0.036 m to the left of the rail base. Therefore, in the NE plots, the trajectory ideally should lie very close to the benchmark points.

While the run trajectories are consistently to the right of the benchmark points, it isn't clear why the distance offset is different between the 5 mph runs and 15 mph runs. However, this difference disappears in the postprocessing with KIPPS, so the distance offset is not very important. Occasionally, the run trajectory is bent during the middle of the run; the GPS system either lost GPS track acquisition in the middle of the run, or it did not have GPS track acquisition until the middle of the run. Fortunately, these runs are usually fixed during postprocessing.

In general, the average error distances between the cold weather and warm weather runs were very similar. Full tables detailing the error distances between the trajectories and benchmark points can be found in *(1)*. The error distances for the raw data were between 18-22 m; after KIPPS processing, these error distances were substantially reduced.

AIRPORT TRAJECTORY RUNS: KIPPS-PROCESSED

Figure 9 and Figure 10 show representative cold weather and warm weather KIPPS-processed trajectories.

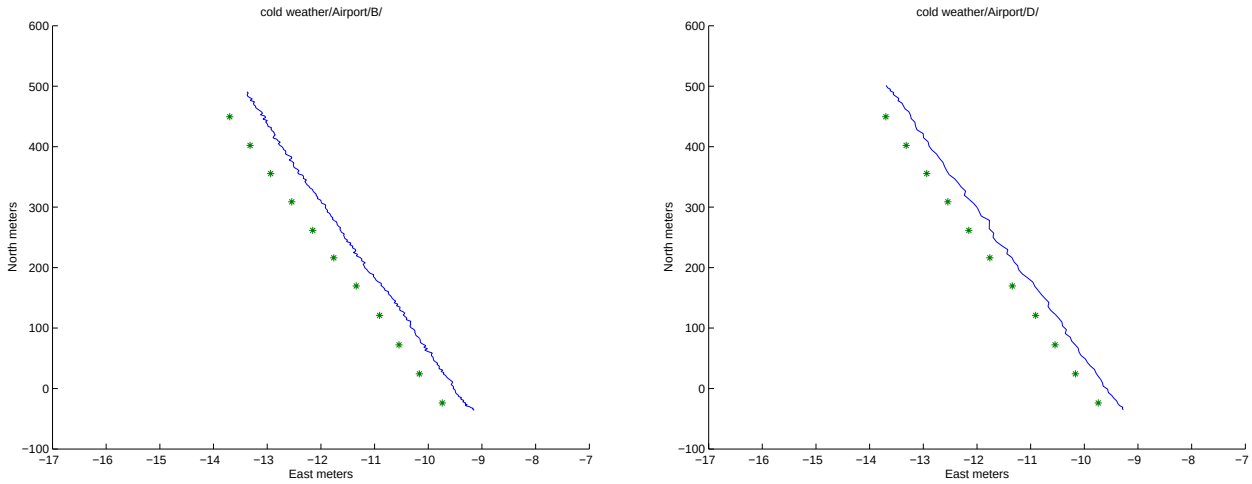

Figure 9 Representative cold weather KIPPS data trajectories, airport runs, (a) 5 mph, and (b) 15 mph

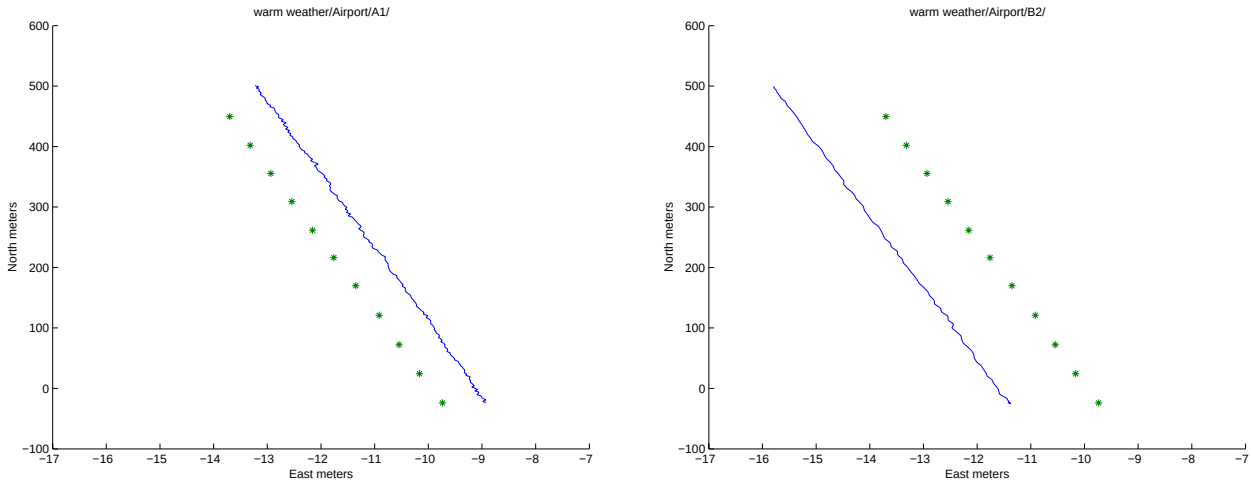

Figure 10 Representative warm weather KIPPS data trajectories, airport runs, (a) 5 mph, and (b) 15 mph

Overall, the KIPPS runs are straighter and closer to the benchmark points. However, the filtered data from the KIPPS navigation solution is not fully consistent with the benchmark points. The KIPPS data should fall almost on top of the benchmark points, but the trajectories lie on both sides of the benchmark points.

In general, the effectiveness of the KIPPS postprocessing depends on when kinematic convergence occurred. Even when the raw data trajectory is misshapen, the filtered run will be straight if kinematic convergnce occurred before the start of the run.

The next four figures show close-up views of raw data trajectories and KIPPS-processed trajectories in the vicinity of 2 benchmark points. The raw data were collected at 0.1 sec intervals while the KIPPS-processed data were determined at 1 sec intervals. The (+) symbols denote an interval of 1 sec during the trajectory run. (Note: 5 mph = 2.2352 m/sec and 15 mph = 6.7056 m/sec.)

Figure 11 shows the raw data and KIPPS trajectory of a 15 mph data run where kinematic convergence occurred before the start of the run. The KIPPS-processed trajectory is significantly straighter than the raw data trajectory; it is also closer to the benchmark points. (The benchmark points are outside the range of Figure 11(a).)

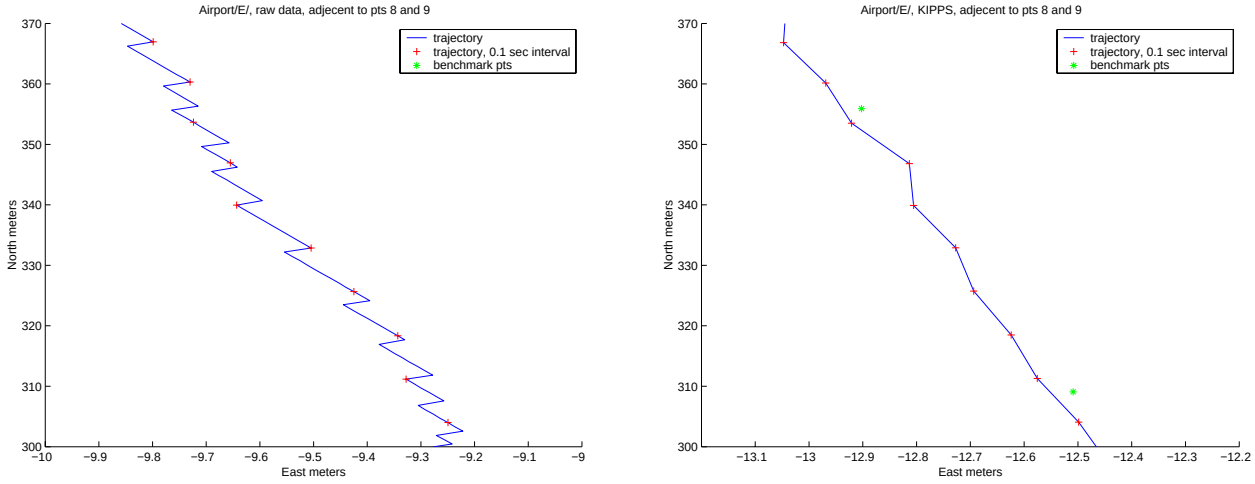

Figure 11 Close-up of Airport Run E (15 mph): (a) raw data, and (b) KIPPS-processed

Figure 12 shows the forward/backward trajectory of the same data run. The backward trajectory was not necessarily collected at 15 mph. In the raw data, the forward and backward raw data trajectories are about 10-15 cm apart, the KIPPS-processed forward and backward trajectories are within 3-4 cm. Thus, once kinematic convergence is achieved, the trajectories over a given section should not vary with one another, at least within a short time frame.

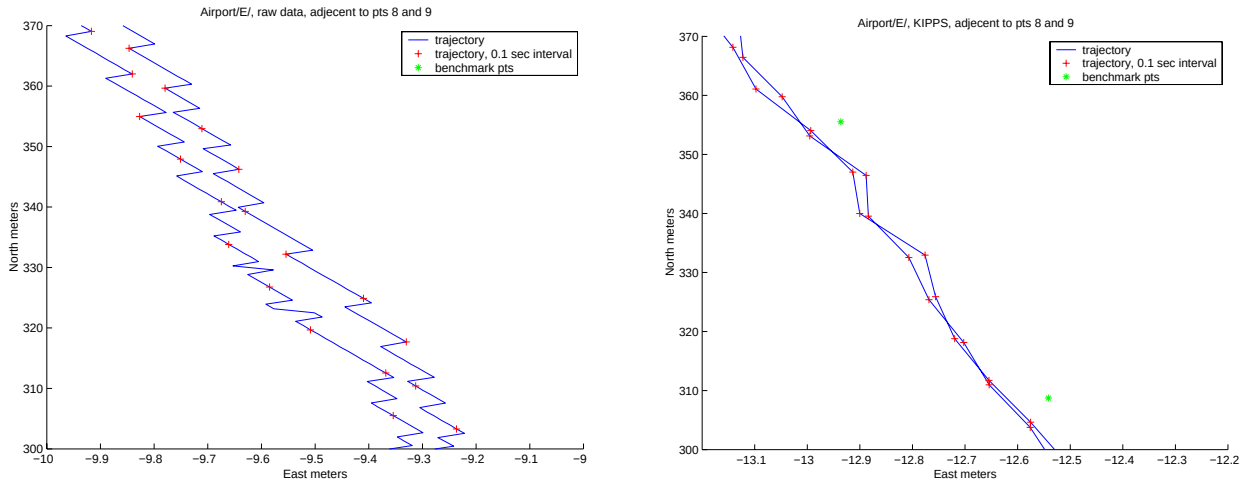

Figure 12 Close-up of Airport Run E (15 mph), forward/backward trajectory: (a) raw data, and (b) KIPPS-processed

LAKE TRAJECTORY RUNS: RAW DATA AND KIPPS-PROCESSED

The lake runs all included a stationary time to calibrate the GPS receiver prior to data collection. Figure 13 shows representative raw data and KIPPS processed trajectories. Taking a closer look at trajectories in the vicinity of three benchmark points, Figure 14 and Figure 15 show that the KIPPS trajectory is superior to the raw data trajectory.

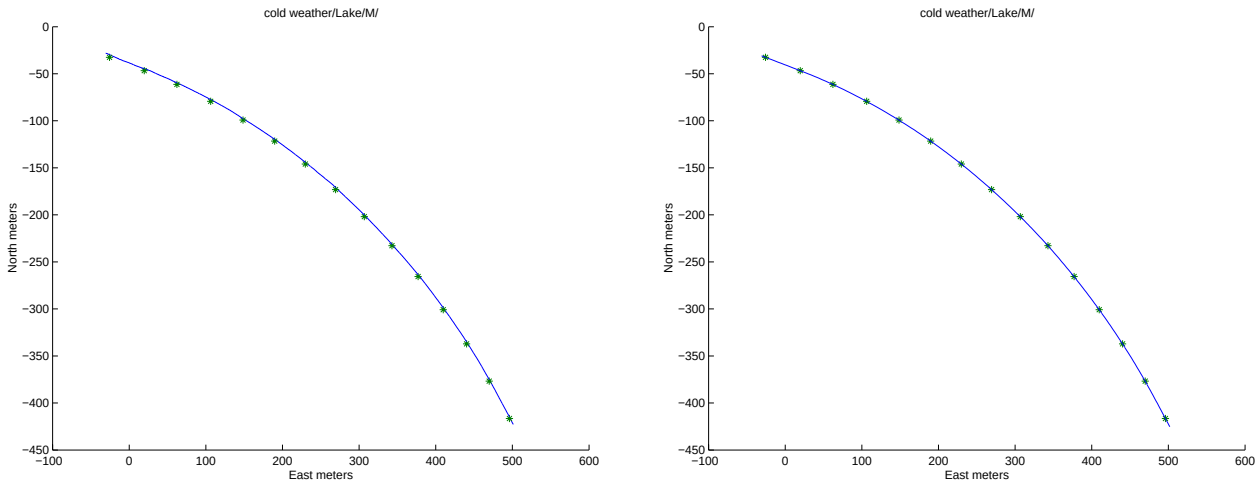

Figure 13 Representative raw data and KIPPS trajectories, lake runs, 5 mph

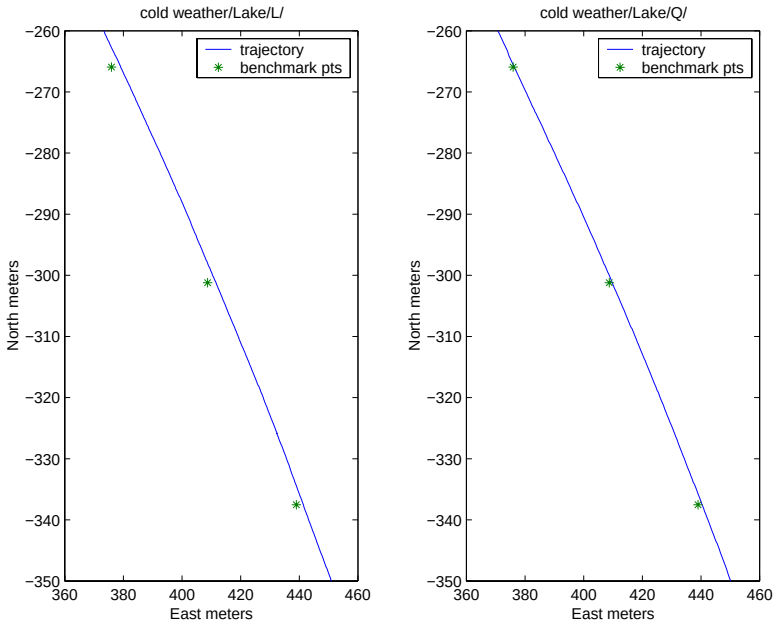

Figure 14 Close-up of raw data trajectories, lake runs, 5 mph (left) and 15 mph (right)

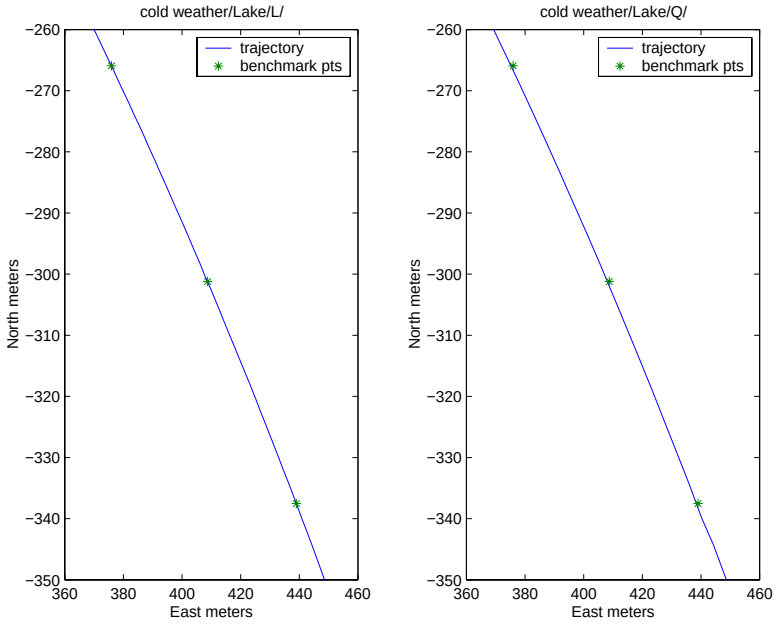

Figure 15 Close-up of KIPPS trajectories, lake runs, 5 mph (left) and 15 mph (right)

As with the airport runs, the quality of the KIPPS lake trajectories depend on whether kinematic convergence was obtained prior to the start of the run. In the next section, we will use a least-squares offset to compensate for the distance offset between the KIPPS trajectories and the benchmark points. We will see that average error distance depends strongly on when kinematic convergence was obtained relative to the start of the trajectory.

DATA PROCESSING

In this section, we consider ways to improve the data trajectories so that they fall closer to the benchmark points. First, we need to devise a way to determine how much the trajectory data needs to be offset. Without the carrier-phase and ambiguity resolution postprocessing, the raw data trajectories are nowhere near the benchmark points. For the KIPPS-processed data, if kinematic convergence does not occur before the run starts, then offsetting the trajectory might help reduce the average offset error. As mentioned below, there are numerous effects that contribute to the offset error. Most

of these could be ameliorated using a more sophisticated experimental procedure and better integer cycle ambiguity resolution. In this study, we bypass these challenges by estimating the offset directly from the kinematic data and the known benchmark locations. Also, it makes sense to smooth the jagged trajectories because rail is inherently smooth. To determine how well a procedure works, we examine the average distance from the closest trajectory data points to the benchmark points. In addition, we compare the error distances of the raw navigational trajectories to the KIPPS-processed trajectories. Unless mentioned, average distance will be 3-D (ECEF or NEU). Sometimes, to measure GPS accuracy on the local tangent plane, 2-D (NE) distance is used.

OFFSET OF KINEMATIC DATA FROM BENCHMARK POINTS

Since the navigation data is based off the GPS antenna on top of the high-railer and the benchmark points are measured from the rail base, an offset distance has to be calculated. Using a physically measured offset distance is problematic; the measurements might not be precise, there is free play (about an inch) between the wheels of the high-railer and the rail itself, and the high-railer cab bounces and sways due to the truck's suspension. Even if the offset distance was precisely measured, because of carrier phase ambiguities, the GPS measurements still may be offset. Thus, as a first look, it makes sense to derive an offset value directly from the measured data using analytical techniques such as minimizing squared error. In the future, this step might be avoided by incorporating a system to automatically measure the position of the high-railer cab with respect to the rail base, and by improving the signal processing algorithms for phase ambiguity resolution.

For the NEU navigation data, each individual test run was first filtered using a basic low-pass FIR digital filter. A FIR filter takes the weighted average of the points surrounding each point in the trajectory; a low-pass filter is essentially a smoother. A variety of filter lengths and coefficients were tested in order to find the optimal filter parameters.

Using the smoothed data run, the closest trajectory point to each benchmark point was determined. Then, for each closest point, a line was fitted through the surrounding trajectory data points using orthogonal regression. This line minimized the sum of the square of the orthogonal distances between these points and the line. The point on the line closest to the benchmark point was said to be the closest orthogonal point.

To determine the offset value, a least squares fit was used to minimize the average squared distance between the closest orthogonal point and respective benchmark point.

The next three figures illustrate this process. In Figure 16, the solid thin line represents the (smoothed) raw data trajectory and the thicker segments on the trajectory represent the line segments to which orthogonal regression was applied.

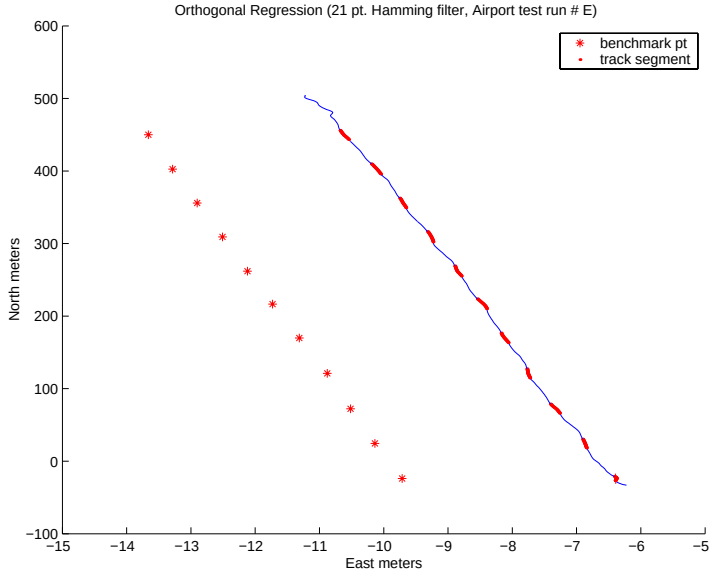

Figure 16 Orthogonal Regression

Figure 17 shows the same plot with a close up view of the track segment between 300 and 318 north meters. In Figure 18, the closest orthogonal points (and original track data run) are shown shifted onto the benchmark points using the least-squares offset value.

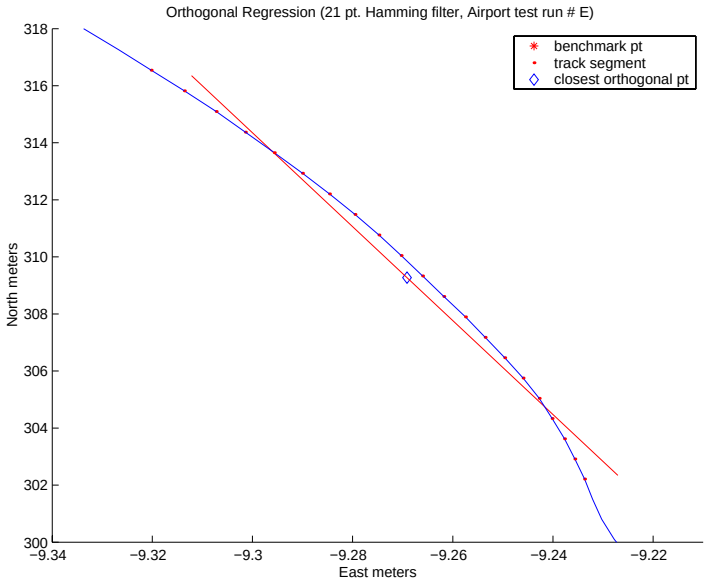

Figure 17 Close-up of orthogonal regression

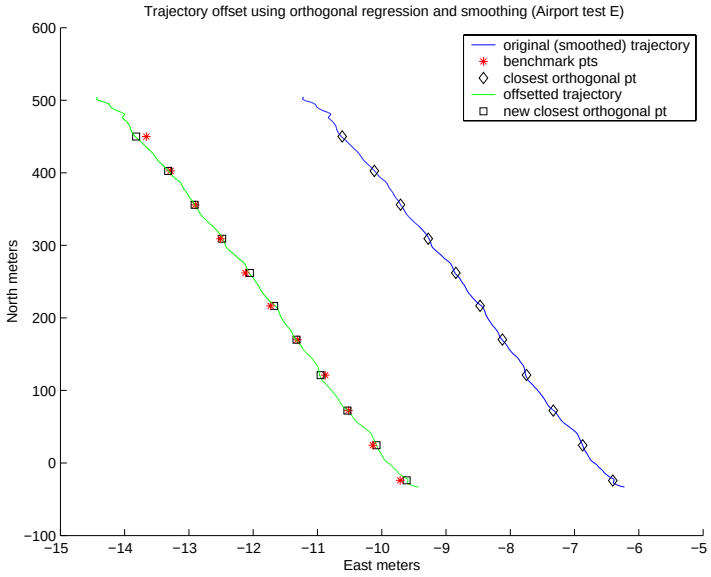

Figure 18 Shifted Trajectory

KIPPS OFFSET CORRECTION

Since the KIPPS data was already filtered, we first looked at offset correction without any additional smoothing of the trajectories. An offset distance was calculated directly from the KIPPS data. Since the KIPPS data has 1/10 the number of data points compared to the raw data, when using orthogonal regression, a line was fitted through fewer points (compared to processing of the raw data) because the points were further spread apart. The rest of the process was the same with both the raw data and KIPPS-processed trajectories; once an optimal offset distance was calculated for each test run, the offset value was added to every data point in that test run. Then, using this offset KIPPS trajectory, the average distance was calculated between the benchmark points and the closest orthogonal trajectory points.

Looking at the cold weather data, Figure 19 shows the performance gain from using offset correction for the airport and lake KIPPS runs. These same improvements (and possibility more) would be afforded by incorporating a system to monitor cab position with respect to the rail, and through improved integer cycle ambiguity resolution. Run A was disregarded because kinematic convergence occurred during the run; the trajectory before convergence is almost 25 m lower in altitude than the rest of the trajectory. Lake runs L-P acquired kinematic convergence prior to the start of the runs. Runs Q and R did worse because kinematic convergence occurred during the run; the trajectories became distorted

when they jumped to another carrier cycle track. For trajectories with very large outlier sections, using a least-squares method could actually increase the average error distance. A more robust method might either assign a separate weighting to the outlying section or disregard it all together. But for these trajectories, with the exception of run A, the current least-squares method works quite well.

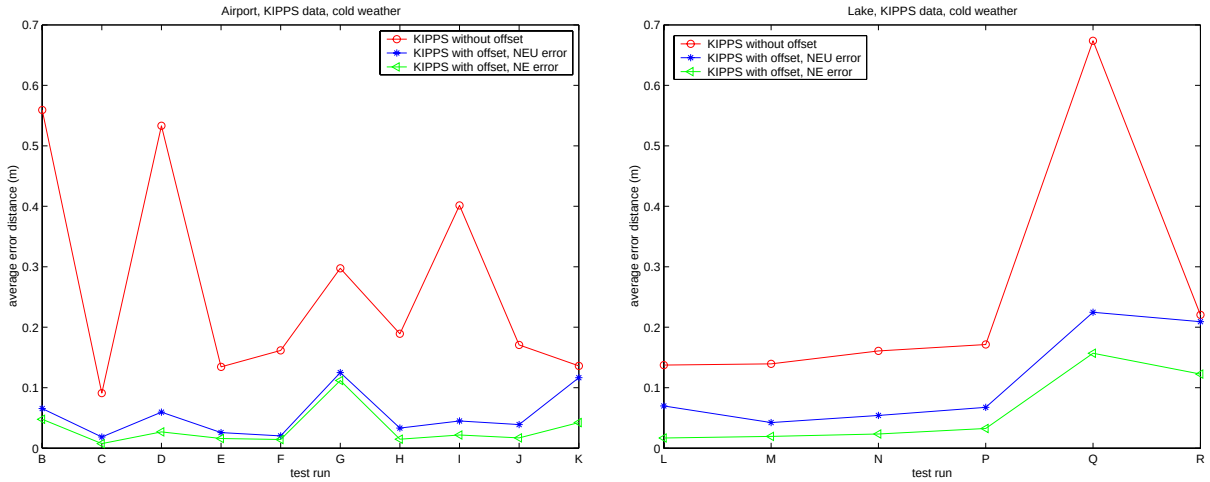

Figure 19 Offset correction of KIPPS trajectories, cold weather, airport and lake runs

Looking at the warm weather data, Figure 20 shows the performance gain for the airport and lake KIPPS runs. Run A4 was disregarded because it is completely erratic; otherwise, the other runs behaved reasonable well. For the lake site KIPPS runs, runs C3, C4, and C5 had large error distances, but after offset correction, the average error distance of run C4 became reasonable.

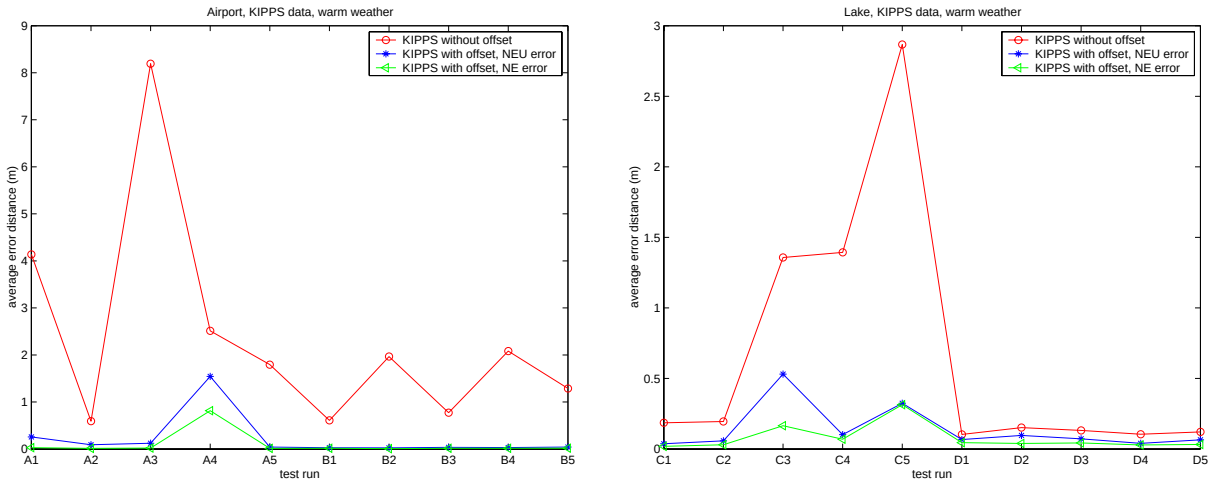

Figure 20 Offset correction of KIPPS trajectories, warm weather, airport and lake runs

Curiously, the error variance without offset correction is significantly greater for the warm weather runs than with the cold weather runs. While cold and warm weather error variances resemble each other after offset correction, we are unsure whether the pre-offset discrepancy is due to measurement errors or the KIPPS software.

But even if this distance offset is incorporated into the data, the NE magnitude is not consistently small, raising questions of repeatability. There are two reasons for this. Kinematic convergence was not always obtained or obtained quickly enough for each run. Runs D, I, and K did not converge, and runs A, B, G, and J converged late. Ideally, the system should have achieved kinematic convergence before the start of any run; unfortunately, kinematic convergence cannot be known until after postprocessing. It is especially odd that runs with stationary times did not converge as quickly or as often as the runs without a stationary time; Rockwell expects that convergence should occur quickly, especially in open areas like the airport and lake test sites. Convergence might be less of a problem for much longer runs, as would occur in a practical application of this technology.

Without kinematic convergence, the system does not necessarily infer the correct number of carrier cycles. Looking at Appendix B in *(1)*, the KIPPS algorithm for runs A and G picked the wrong track at the beginning. It eventually snapped to the correct track, but too late for the data to be useful. It is not guaranteed that after picking the correct track, KIPPS remains with the track and not move to an erroneous track. For runs C, E, F and H, KIPPS obtained kinematic convergence before the start of the run, and remained locked onto the correct carrier cycles. These runs have average error distances within 5-7 cm before offset and 1-2 cm after offset in the NE coordinate frame. Thus, under ideal conditions, it seems possible to generate very accurate trajectories.

As mentioned before, ICAR is not a fully solved problem. This ambiguity generally manifests itself as a constant bias for systems without sudden velocity changes. While this issue needs to be studied further, for our analysis, we simulate removal of this bias by using a least-squares fit between the trajectory and benchmark points.

SMOOTHING OF KIPPS TRAJECTORIES BEFORE OFFSET CORRECTION

In this section, we examine the performance of KIPPS trajectory smoothing for reducing average error distance. We considered various FIR filters and filter lengths to determine what performance gains could be achieved.

As mentioned before, a FIR low-pass filter takes a weighted average of points around a center point. A filter of length N is referred to as an N-point filter. We used three filters: rectangular, triangular, and Hamming. A rectangular filter averages the points with equal weights. A triangle filter gives the center point the largest weight, with the weights decreasing linearly from the center point. A Hamming filter lies in between the two, with the weights resembling a cosine wave. We examined other filters, but their performance was very similar to the three described above.

For a representative airport run, Figure 21 shows the average error distance verses filter length for the three types of FIR filters.

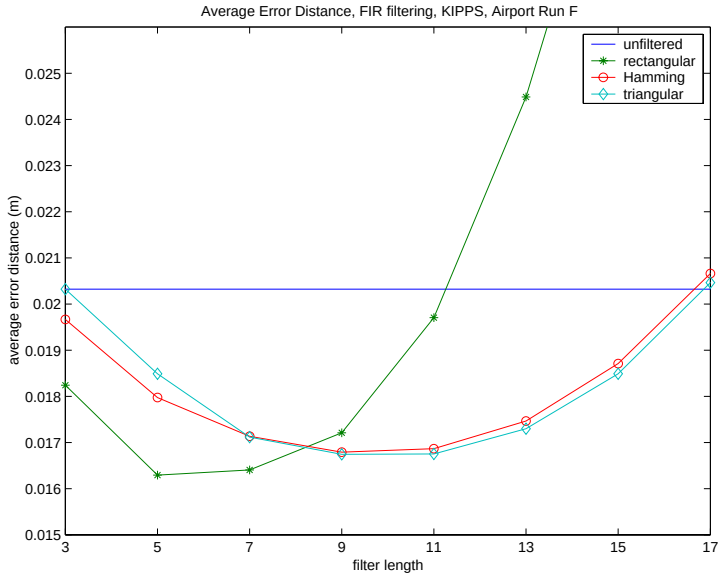

Figure 21 Average error distance using various FIR filter lengths, KIPPS, airport run F

Looking at the KIPPS airport runs, Figure 22 shows the average error when using a Hamming filter; similar results hold when using a rectangular filter and triangular filter. Note that since the KIPPS data was processed at 1 Hz, the FIR filter length corresponds to 1 seconds in trajectory length. For example, a 5-pt filter takes the weighed average of 5 seconds of trajectory data around a center point. Thus, the optimal filter length for the 5 mph runs is generally larger than for the 15 mph runs.

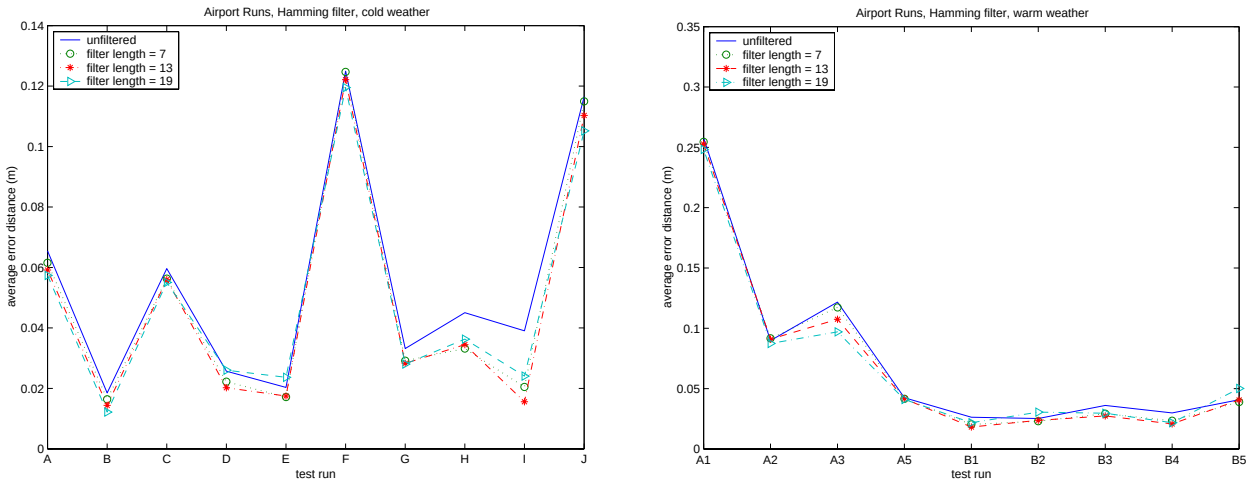

Figure 22 Average error distance using Hamming filter, (a) cold weather and (b) warm weather, KIPPS, airport run

For the airport runs, as long as the filter length was reasonable, the average error distance decreased. But, for most runs, the average error distance did not decrease more than 0.5-1.5 cm. In general, the FIR filters offered performance gains similar for both cold and warm weather runs. An exception was run A3, which seemed to benefit greatly from FIR filtering. This is somewhat misleading because the FIR improvement in the local NE plane was less than 0.5 cm, meaning that most of the performance gain came from smoothing the altitude data.

The same data processing procedure was followed using the lake site data runs. Unfortunately, for a curved trajectory, filtering often increased the average error distance. For a representative lake run, Figure 23 shows the average error distance verses filter length for the three types of FIR filters.

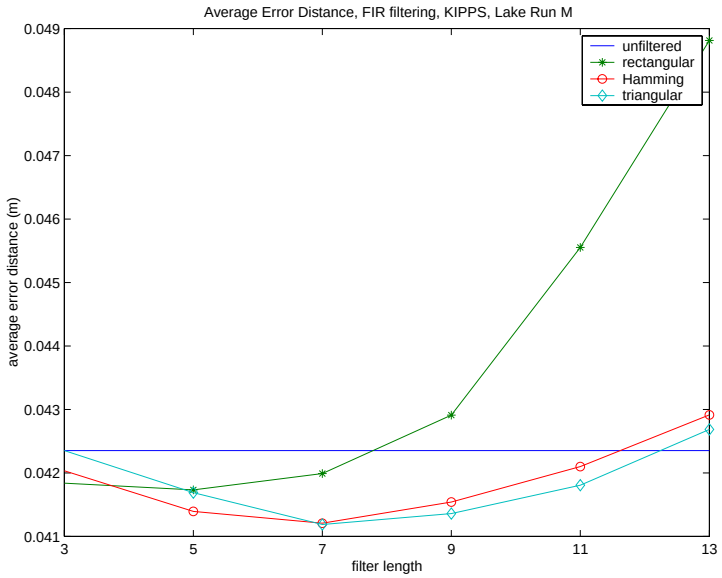

Figure 23 Average error distance using various FIR filters, KIPPS, lake run Q

As the filter length increased, the average error distance increased, after a very slight decrease. Because the lake trajectory is curved, simple FIR smoothing effectively moved the trajectory inwards, making the trajectory curve smaller. The triangular and Hamming filters did not perform as badly as the rectangular filter because they weighted the center point the most; however, these filters were not very useful. Looking at the KIPPS lake runs, Figure 24 shows the average error when using a Hamming filter for various filter lengths; similar results hold when using a rectangular filter and triangular filter.

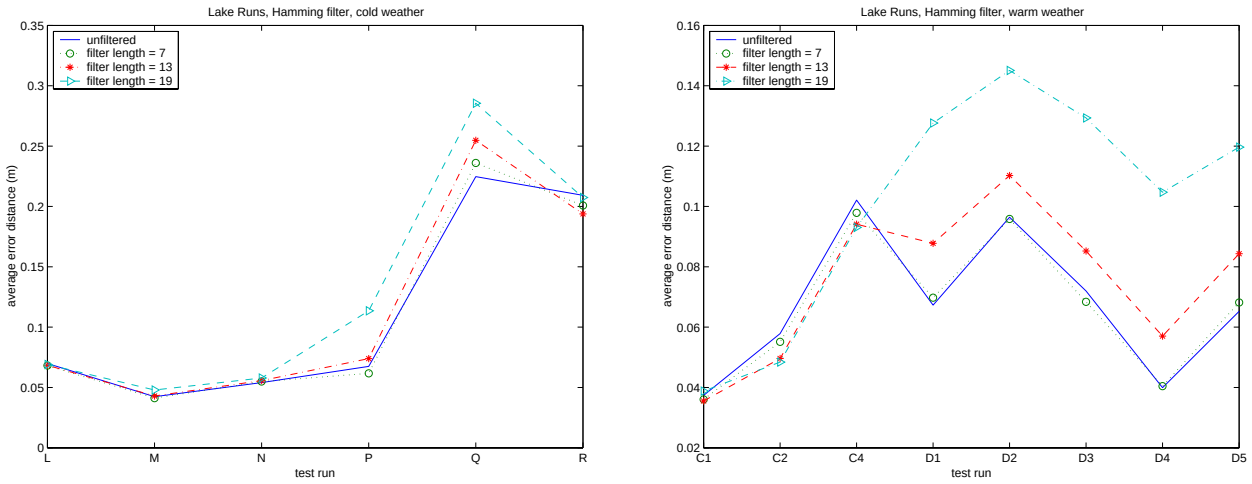

Figure 24 Average error distance using rectangular filter, (a) cold weather and (b) warm weather, KIPPS, lake run

The lake results illustrate that while there can be room for improvement in the filter or tracking design, a simple FIR filter is not sophisticated enough for this trajectory shape. Note that even if the KIPPS trajectories were smoothed after offset correction, the results would be very similar to those discussed in this section, since the ordering of processes does not address the limitations of FIR filtering itself.

SMOOTHING OF RAW DATA TRAJECTORIES BEFORE OFFSET CORRECTION

In the previous section, the trajectories to be smoothed were outputs of KIPPS, which had already applied both ICAR and Kalman filtering. To test the effectiveness of KIPPS, we also applied the FIR smoothing procedure directly to the raw data trajectories.

For a representative airport run, Figure 25 shows the average error distance verses filter length for the three types of FIR filters. In general, it seems that as long as the length of the FIR filter was reasonable, the average error distance can consistently decrease to within a few centimeters. There was not much difference between the various filter types.

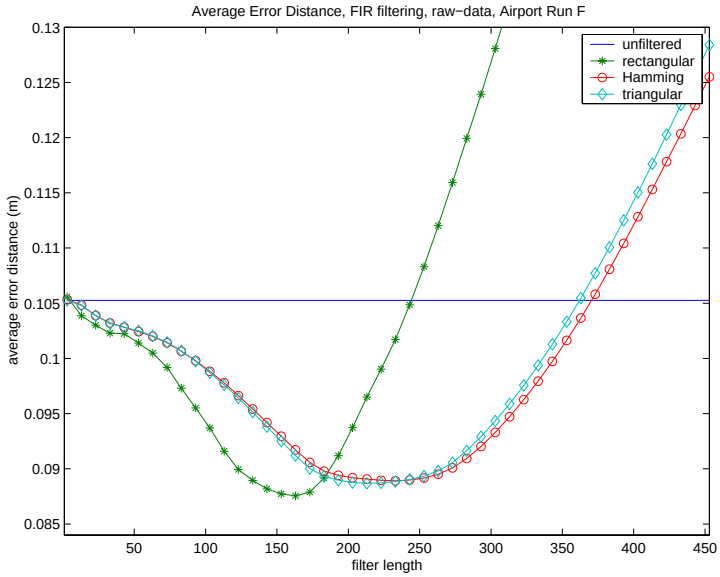

Figure 25 Average error distance using various FIR filters, raw data, Airport Run F

Figure 26 shows the average error distance when using a Hamming filter for the cold weather and warm weather airport runs. The error did not decrease significantly. For the most part, the average error distances did not fall below 10 cm. Run H did the worst because the GPS system either lost GPS track convergence in the middle of the run, or it did not have GPS track convergence until the middle of the run.

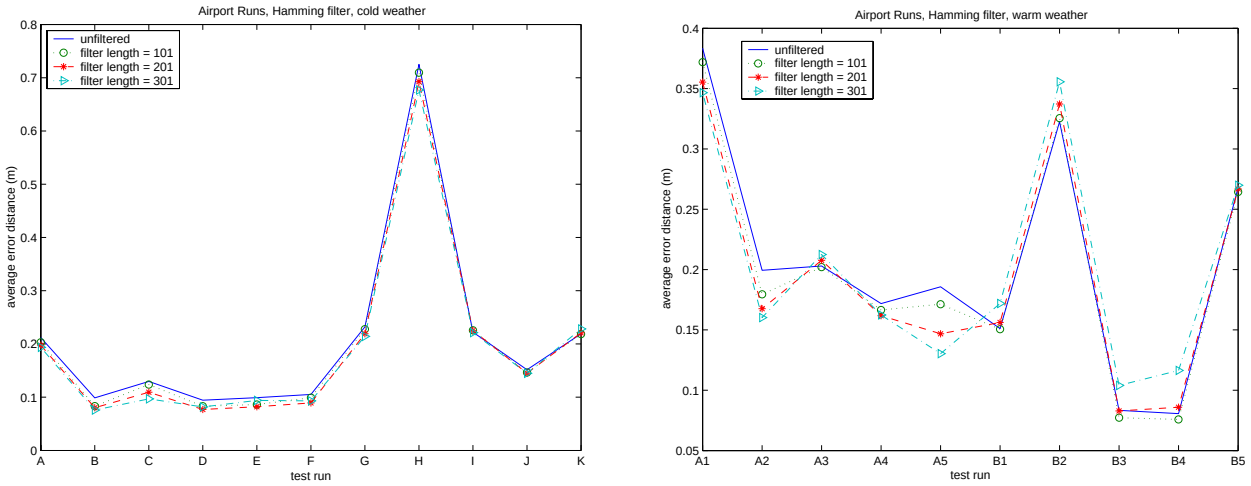

Figure 26 Average error distance using Hamming filter, (a) cold weather and (b) warm weather, raw data, airport runs

The same data processing procedure was followed using the lake site data runs. While filtering was helpful, the average error distance was much larger than for the airport data. Changing filter types and lengths did not help. For a representative lake run, Figure 27 shows the average error distance verses filter length for the three types of FIR filters.

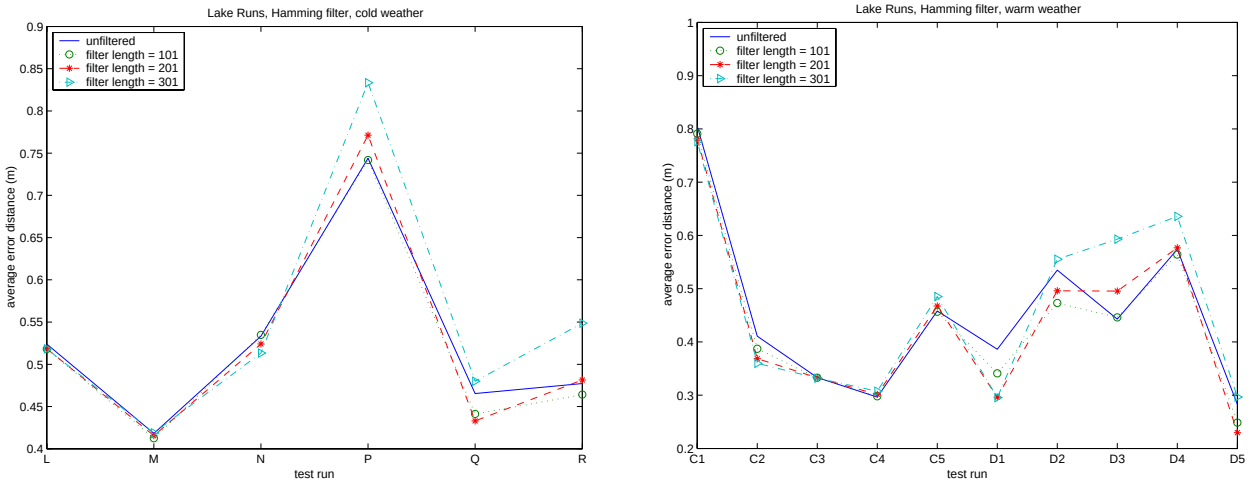

Figure 27 Average error distance using Hamming filter, (a) cold weather and (b) warm weather, raw data, lake runs

Even though filtering offered little improvement when applied to the raw data, this exercise is still useful because it shows that a more sophisticated filtering method is necessary for curved track.

OTHER DATA PROCESSING METHODS

We also explored other signal processing methods to improve the accuracy of the rail trajectories. A full description of methods used can be found in *(1)*. However, these methods do not resolve the phase ambiguity problem or the need for more elaborate GPS error reduction methods. That work will involve a deeper understanding of the GPS system itself in order to resolve potential error sources from the receiver, as well as account for the characteristics of the vehicle platform and rail. Until then, a practical GPS rail measurement system is still relatively far off. But once a more reliable GPS system is developed, finding practical parameters for these signal processing techniques should become easier.

ANALYSIS OF RAIL BUCKLES

According to Andrew Kish, a rail buckle expert from VOLPE in Cambridge, MA, the ability to detect incipient buckles has been one of the most challenging R&D concerns since the advent of continuous wielded rail (CWR), with only limited success to date. Most of the detection methods are based on measuring the longitudinal force in the rails, which then could be indicators of potential buckling prone conditions.

Rather than being preceded by a visible geometric distortion of the rail that builds up slowly over time, buckles generally occur suddenly and under the train without warning, often resulting in serious derailments. There are some instances when the resulting buckle under the train occurs toward the end of the consist, with the last few cars making it over the buckled misalignment without derailing and leaving a large buckle misalignment in the track. In many cases, this buckle is not detected before the arrival of the next train, which can derail if the engineer can't stop or slow the train before coming upon the buckle. A GPS system attached to the end of the buckle-inducing train could potentially detect these buckles right after they develop.

Approximating the buckle as a sinusoid seems reasonable since there are several mode shapes possible. Tangent (straight) track tends to buckle out in mode shape 3, while curved tracks buckle in mode shape 1. The buckled wavelengths typically vary from 25 to 50 meters, with amplitudes of 10 cm to 50 cm, depending on the compressive force in the rails and on track curvature.

One of our goals was to determine how well a GPS system could detect potential buckles for various buckle amplitudes. Because the output of the GPS KIPPS postprocessing has measurement error on the average of 2-5 cm, the system might not always be able to detect a potential buckle. However, there are powerful statistical detection procedures available for such problems. We present a quantitative approach to buckle detection using detection criteria found in the signal processing and communication theory literature.

BUCKLE MODELING

For this analysis, we model a potential rail buckle as a sinusoidal wave. The assumed buckle length is 50 m, with a GPS data point collected every 5 meters. Given a buckle amplitude, we can add measurement noise to each data point. The measurement error is modeled as Gaussian noise. This noise is composed of independent and identically distributed (iid) random variables, where the standard deviation is σ cm and the variance is σ^2 cm^2. The noise models the uncertainty in our GPS measurements. Figure 28 shows the rail geometry with and without corrupted additive noise.

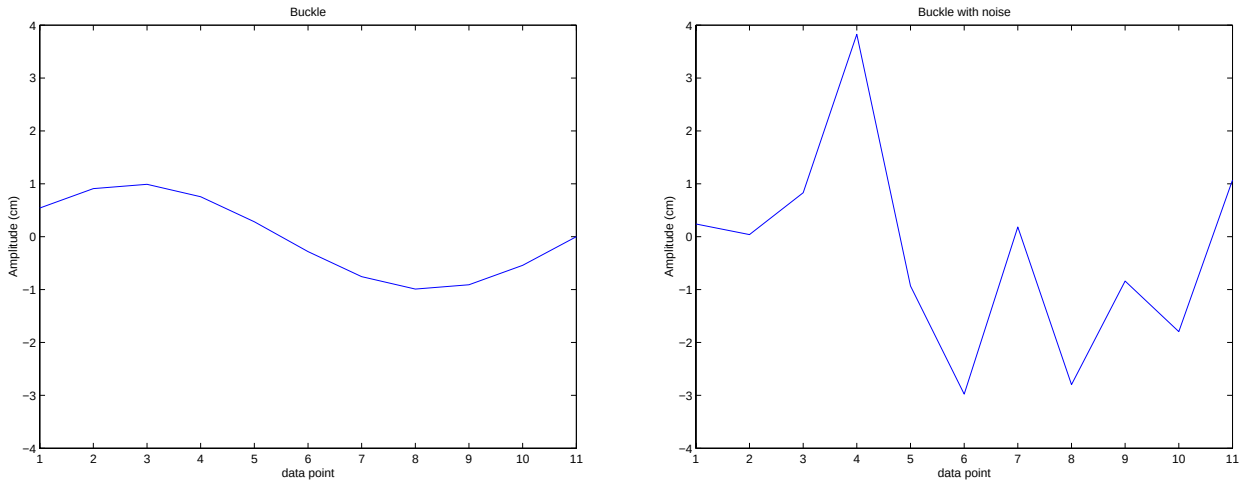

Figure 28 Buckle model (a) without noise, and (b) with noise

Using advanced signal processing techniques often found in communication and probability theory, we can use hypothesis testing to determine how well we can detect a buckle. The full mathematical description of this technique can be found in *(1)* and *(4)*; this is often called a *maximum likelihood test*.

Our objective is to understand how well we can detect a buckle using the GPS measurements. Let P_F be the probability of false alarm (i.e. we say the buckle is present when it is not) and P_D be the probability of detection.

We want to compare P_D with P_F. We can use the characteristics of the buckle amplitude and noise variance to create a plot of P_D versus P_F. This curve is referred to as the receiver operating characteristic (ROC). The figures below describe the ROC for A = 2, 5, 10 cm for σ^2 = 4, 9, 25 cm^2. Curves that nearly touch the upper left corner in the plots correspond to desirable situations where high detection probability and low false alarm probability are available simultaneously.

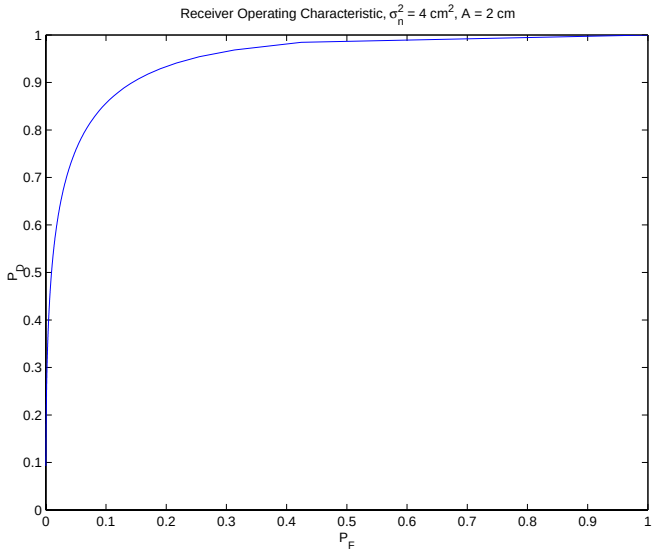

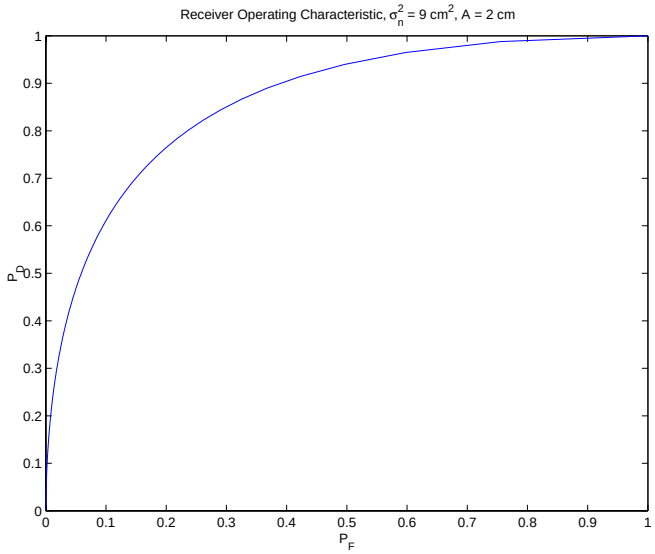

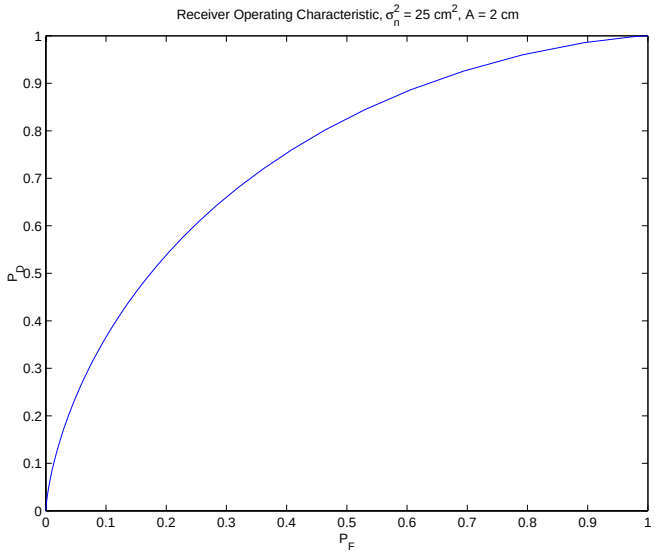

Figure 29 Receiver operating characteristic, P_F versus P_D for $\sigma^2 = 4, 9, 25$ cm^2, A = 2 cm

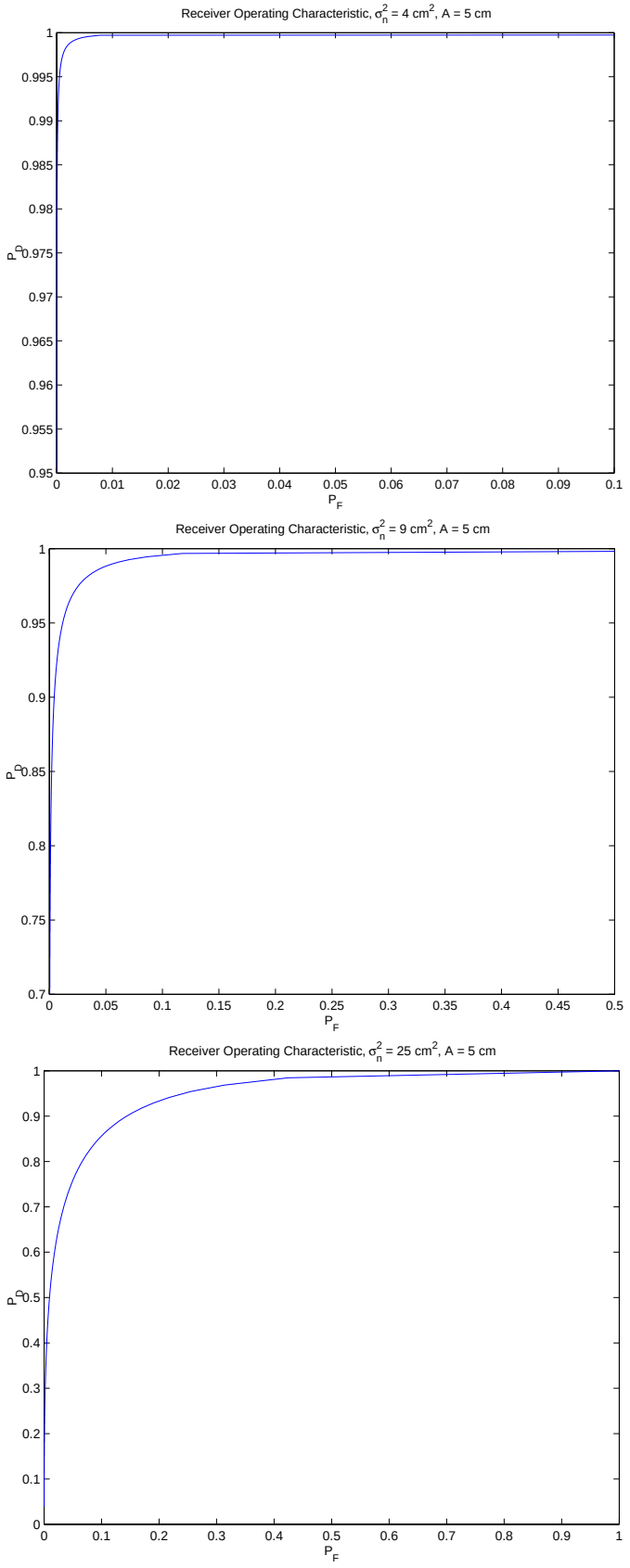

Figure 30 Receiver operating characteristic, P_F versus P_D for $\sigma^2 = 4, 9, 25$ cm^2, A = 5 cm

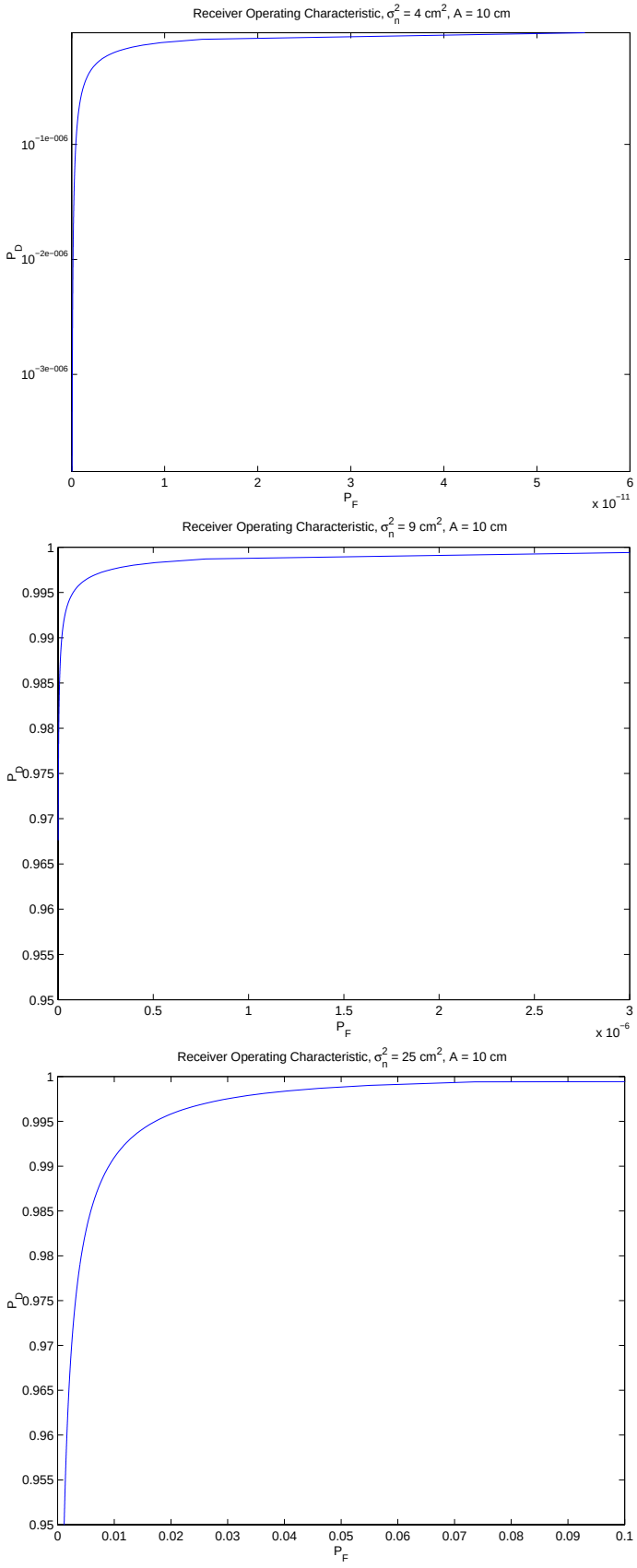

Figure 31 Receiver operating characteristic, P_F versus P_D for σ^2 = 4, 9, 25 cm^2, A = 10 cm

As the noise variance increases, the ROC plot rises less steeply. Likewise, as the signal amplitude increases, the ROC plot rises more quickly. We see that for a developing rail buckle with an amplitude of 1 cm (across 50 m) and noise variance of 25 cm^2, buckle detection would be difficult. However, if the buckle amplitude is a bit larger, the detection probability improves dramatically. Of course, reducing GPS measurement noise increases the likelihood of detecting small amplitudes.

Having a small probability of false alarm is important for detection repeatability. In practice, many sections of track would be examined by a working system. For example, if P_F is 0.1 and 100 sections of track were examined, the processor might mistakenly identify 10 sections as having buckles. Practical considerations would be important in determining a tolerable P_F. For A = 2, we see from Figure 29 that hypothesis testing based on kinematic GPS data would not provide a high enough P_D for $P_F << 0.1$. However, for A =5, Figure 30 shows that very high P_D is theoretically achievable for $P_F << 0.1$ for $\sigma_n^2 = 4$ and 9, which corresponds to GPS errors having standard deviations 2 cm and 3 cm, respectively. In Figure 31, with A = 10 cm, we see that high P_D and low P_F are simultaneously achievable, even for the case $\sigma_n^2 = 25$, which corresponds to a GPS error with standard deviation = 5 cm.

ACCOMPLISHMENTS AND FUTURE RESULTS

Success in measuring rail position using high-precision GPS depends on questions dealing with position, planning, and system integration. This research furthered the work in these areas by field testing and benchmarking a sophisticated GPS system for measuring rail position from a moving platform. Additionally, issues in GPS processing, trajectory analysis, and buckle detection were addressed. We give a brief summary here of the accomplishments presented in this report, and suggest further work motivated by our research.

Using differential GPS, we were able to obtain reasonably accurate data from a moving platform at speeds up to 15 mph. The GPS trajectories were compared to a set of benchmark points. This work primarily focused on providing a detailed analysis of the postprocessed KIPPS trajectories. Error analysis using different trajectories and vehicle speeds were presented, showing that high accuracy on the order of 10 cm is possible with kinematic convergence.

Various signal processing techniques were presented which compensate for trajectory bias and jaggedness. Smoothing solutions based on FIR filtering and interpolating splines were shown to decrease error distance with varying effectiveness, depending on trajectory shape and KIPPS postprocessing. The report identifies tradeoffs for each signal processing technique, depending on the scenario.

Finally, a buckle detection model was presented for determining the feasibility using GPS measurements to detect small-amplitude incipient rail buckles. Initial calculations showed promise in measuring small buckle amplitudes in the presence of GPS measurement noise. Currently it is unknown whether such small-amplitude precursors exist prior to development of the full rail buckle.

The success of high-precision GPS depends on developing better processing algorithm to improve repeatability of measurements. At the outset of the study we had thought that the Kalman filter in KIPPS was in need of redesign. However, the major issue with KIPPS turned out to be the need for better integer cycle ambiguity resolution. In order to satisfy the error parameters needed for repeatable high-accuracy measurements, improvements to ICAR are needed. For some purposes, a constant trajectory offset may not be objectionable if the shape of the trajectory is accurate. If kinematic convergence occurs during a run, it will distort the trajectory shape, but suitable postprocessing could easily correct for this. For situations where we desire to know absolute rail position, within 5 or fewer cm, future work must address the ICAR problem. It will be necessary to research the GPS literature on this topic to see what improvements might be made. ICAR is a version of a mathematical problem known as phase unwrapping in the signal processing literature. In the past few years, promising new approaches to phase unwrapping have been developed *(5)*. In the future, it would be worthwhile to modify those techniques for solution of the ICAR problem and to assess the resulting performance. In a few years, the addition of a new civilian GPS frequency will help simplify this problem.

In another area of future research, the current test set-up should be modified by adding an optical reader that could signal the GPS unit at the instant that a mark placed on the side of the rail had been passed. Having this capability would provide a means of measuring absolute position of such marks, which could be used to detect rail slippage down a mountainside, or to measure the expansion or contraction of the rail between two marks. Expansion/contraction measurements, together with current rail temperature and neutral temperature, would permit calculation of rail stress, and perhaps the prediction of rail buckles and breaks.

More knowledge is needed about development of rail buckles. Our calculations show that a 50 m incipient buckle having amplitude 5-10 cm could be very reliably detected using kinematic GPS. We are uncertain, though, whether this capability would be useful in practice. The sizes of any possible geometric precursors to rail buckle need to be determined.

Finally, we point out that rail position could be measured with extraordinary accuracy by using stationary (versus moving) GPS. For some purposes, it may be prudent to develop a fixture, easily attached to the rail, from which a GPS

unit could provide resolution on the order of 2-3 mm with just a few minutes of data collection per fixture location. Such an approach would provide for accurate measurement of rail stress and also could identify nearly any geometric precursor to a rail buckle.

APPENDIX A: ANTENNA CALIBRATION

For kinematic positioning, the GPS antenna on the roof of the high railer had to be referenced to the IMU. The location of the IMU relative to the antenna phase center is called the antenna lever arm, and is needed by the GPS software to combine the GPS and IMU measurements. Table 6 provides the lever arm from the IMU to the GPS antenna phase center on the high-railer. The antenna was behind, above, and to the right of the IMU.

Component	Length (cm)	Accuracy (cm)
X	-43	±1
Y	77	±1
Z	-94	±1

Table 6 Antenna Lever Arm

The phase center of the antenna refers to the location computed by the GPS software and is determined through a set of calibration measurements. The phase center height of the antenna located at the base station was different from the phase center height of the antenna located at the survey point. As Figure 32 shows, the phase center height is measured up from the top of the center pole.

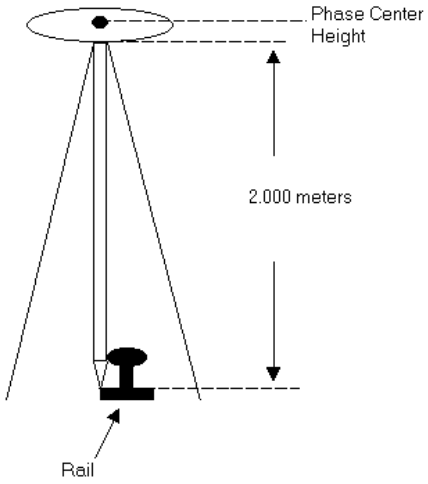

Figure 32 Survey Antenna Diagram

Table 7 shows the phase center heights, referenced from the top of the center pole.

GPS Unit	Type	Phase Center Heights (cm)*
Base Station	Ashtech 700718B	8.39
Benchmark Location	Ashtech 700700C	5.15

*Source: NGS Antenna Calibration Data

Table 7 Phase Center Heights

The distance from the phase center of the antenna to the rail base was subtracted to obtain the coordinates of the benchmark and base points. All references in this report use the corrected heights for the benchmark and base points.

BIBLOGRAPHY

(1) J. Lee, *Estimation of Rail Position and Geometry Using High-Precision Differential GPS*, M.S. thesis, University of Illinois, Urbana-Champaign, 2003.

(2) E. D. Kaplan, Ed., *Understanding GPS: Principles and Practice.* Artech House, Inc., 1996.

(3) B. Hofmann-Wellenhof, H. Lichtenegger, and J. Collins, *GPS - Theory and Practice, 5th ed.* Springer-Verlag Wien New York, 2001.

(4) H. L. V. Trees, *Detection, Esimation, and Modulation Theory, Part I.* John Wiley & Sons, Inc., 1968.

(5) L. Ying, B. J. Frey, R. Koetter, D. C. Munson, Jr. A Dynamic Programming Approach to 2-D Phase Unwrapping. *Proc. IEEE Int. Geoscience and Remote Sensing Symp.*, Toronto, Canada, June 2002.